Supporting Information

Understanding and manipulating the intrinsic point defect in α-MgAgSb for higher thermoelectric performance

Zihang Liu[ab], Huiyuan Geng[c], Jun Mao[bd], Jing Shuai[b], Ran He[b], Chao Wang[e], Wei Cai[a], Jiehe Sui[*a], and Zhifeng Ren[*b]

[a] National Key Laboratory for Precision Hot Processing of Metals, School of Materials Science and Engineering, Harbin Institute of Technology, Harbin 150001, China. *E-mail: suijiehe@hit.edu.cn

[b] Department of Physics and TcSUH, University of Houston, Houston, TX 77204, USA. *E-mail: zren@uh.edu.

[c] State Key Laboratory of Advanced Welding and Joining, Harbin Institute of Technology, Harbin 150001, China.

[d] Department of Mechanical Engineering, University of Houston, Houston, TX 77204, USA.

[e] State key lab of electronic thin film and integrated device, University of Electric Science and Technology of China, Chengdu 611731, China.

Experimental section

Synthesis. Mg (99.98%; Alfa Aesar), Ag (99.99%; Sigma Aldrich), and Sb (99.999%; Alfa Aesar) were weighed according to the nominal composition $MgAg_{0.97}Sb_{0.99}$ and then loaded into the stainless steel jar in a glove-box under argon atmosphere. The two-step ball milling process was identical to our previous reports and finally the ball-milled powder was loaded into a graphite die and hot pressed at different temperatures (533 K, 553 K, 573 K, 593 K, and 613 K) for 5 min under a pressure of 80 Mpa.[1-6] The as-pressed discs were then annealed at 523 K in air for 30 min prior to structure characterizations and property measurements.

X-ray diffraction and Electron Microscopy. X-ray diffraction (XRD) analysis was performed using a PANa-lytical multipurpose diffractometer with an X'celerator detector (PANalyticalX'Pert Pro). The phases were analyzed with JADE 6.0 software and Rietveld refinements. The microstructure was observed by a scanning electron microscope (SEM, JEOL 6330F).

Physical Property Characterizations. Bar samples were cut from the disks and used for simultaneous measurement of electrical resistivity (ρ) and Seebeck coefficient (S) on a commercial system (ULVAC ZEM-3). The thermal conductivity was calculated using $\kappa = DC_p d$, where D, C_p, and d are the thermal diffusivity, specific heat capacity, and density, respectively. The thermal diffusivity (D) was measured using the coin sample on a laser flash system (Netzsch LFA 457, Germany). The specific heat capacity (C_p) was measured on a differential scanning calorimetry thermal analyzer (Netzsch DSC 404 C, Germany). The density (d) of all the samples are around 6.2 g cm^{-3}, determined by the Archimedes method. The Hall coefficient R_H at room temperature was measured using the PPMS (Physical Properties Measurement System, Quantum Design). The carrier concentration (n_H) was obtained by $n_H =$

$1/(eR_H)$ and the carrier mobility (μ_H) was calculated by $\sigma = e\mu_H n_H$, where e is the electronic charge and σ the electrical conductivity.

Electronic calculation of pure α-MgAgSb. The electronic structure of the pure, well-ordered α-MgAgSb was calculated by the density-functional theory (DFT) as implemented in the open-source Quantum Espresso program package.[7] We used the projected augment wave (PAW) potentials, provided by the standard solid-state pseudo potential library. The exchange-correlation function was taken within the generalized gradient approximation (GGA) in the parameterization of Perdew–Burke–Ernzerhof (PBE).[8] A plane-wave basis is adopted for the expansion of the valence electron wavefunctions with kinetic-energy cutoffs of 50 Ry. For ground state calculations we use an 8×8×8 Monkhorst–Pack k-point mesh. Besides, the spin–orbit couplings were not included in the current calculations.

Electronic calculation of disordered α-MgAgSb. The electronic structure calculations of defected α-MgAgSb compounds have been performed by means of the scalar relativistic Korringa–Kohn–Rostoker (KKR) method as implemented in the AkaiKKR (machikaneyama) program package.[9, 10] The coherent potential approximation (CPA) was used to determine the coherent t-matrix in the effective medium.[9, 10] Therefore, the KKR–CPA method allows accounting for disorder effects in the self-consistent way.

The calculations were performed in the scalar relativistic mode by solving the Dirac equation for core and valence states. Moruzzi, Janak, and Williams (MJW) method was used for the parameterization of the exchange energy.[11] The k-integration mesh was set to a size of (7× 7 × 7) during the self-consistent cycles (213 k-points in the irreducible wedge of the Brillouin zone). The Mg and Sb atoms are placed on the 16i Wyckoff positions; the Ag atoms are placed on the 4a, 4b, and 8e positions. The crystal potential of vacancy was converged self consistently as for other atoms, except for an assumption of no nuclear charge (Z = 0). The self-consistency cycles were repeated until input–output differences of the potentials and charges inside the muffin-tin spheres were of the order of 1 mRy and 10^{-3} e, respectively.

3

Calculation of the formation energies. For ordinary semiconductors, the formation energy difference between charged and neutral defects is usually small.[12, 13] We, thus, only consider the formation energy of neutral defect in α-MgAgSb. The formation energy of defects is expressed as:

$$\Delta H_f(\chi) = \Delta E(\chi) + n_{Mg}\mu_{Mg} + n_{Ag}\mu_{Ag} + n_{Sb}\mu_{Sb} \tag{1}$$

where

$$\Delta E(\chi) = E(\chi) - E(MgAgSb) + n_{Mg}E_{Mg}^{solid} + n_{Ag}E_{Ag}^{solid} + n_{Sb}E_{Sb}^{solid} \tag{2}$$

Here, $E(\chi)$ is the total energy of a crystal containing the defect, $E(MgAgSb)$ is the total energy for the same crystal in the absence of the defect, the n's are the numbers of Mg, Ag, and Sb atoms transferred from the crystal to the reservoirs in forming the defect alloy, the E_s^{solid} are the ground state energies in the solid state, and the μ's are the chemical potentials referenced to E_s^{solid}.

Since the formation of defects relates to the synthesis or heat-treatment conditions, the formation energy must depend on the chemical potentials, reflected by the environment. The chemical potential μ is bounded by the following thermodynamic limits:

(i) The μ's must be lower than the ground-state energies E_S^{solid} to prohibit the precipitation of solid elemental Mg, Ag, and Sb, so that

$$\mu_{Mg} \leq 0, \quad \mu_{Ag} \leq 0, \quad \mu_{Sb} \leq 0 \tag{3}$$

(ii) The μ's must result in a stable α-MgAgSb structure, so that

$$\mu_{Mg} + \mu_{Ag} + \mu_{Sb} = \Delta H_f(MgAgSb) = -331.8304\,\text{Ry} \tag{4}$$

(iii) The μ's must not result in the formation of impurity phases, so that

$$3\mu_{Ag} + \mu_{Sb} \leq \Delta H_f(Ag_3Sb) = -318.2891\,\text{Ry} \tag{5}$$

$$3\mu_{Mg} + 2\mu_{Sb} \leq \Delta H_f(Mg_3Sb_2) = -664.2572\,\text{Ry} \tag{6}$$

[1] H. Zhao, J. Sui, Z. Tang, Y. Lan, Q. Jie, D. Kraemer, K. McEnaney, A. Guloy, G. Chen, Z. Ren, Nano Energy 2014, 7, 97.

[2] J. Shuai, H. S. Kim, Y. Lan, S. Chen, Y. Liu, H. Zhao, J. Sui, Z. Ren, Nano Energy 2015, 11, 640.

[3] J. Sui, J. Shuai, Y. Lan, Y. Liu, R. He, D. Wang, Q. Jie, Z. Ren, Acta Materialia 2015, 87, 266.

[4] D. Kraemer, J. Sui, K. McEnaney, H. Zhao, Q. Jie, Z. Ren, G. Chen, Energy & Environmental Science 2015, 8, 1299.

[5] Z. Liu, J. Shuai, J. Mao, Y. Wang, Z. Wang, W. Cai, J. Sui, Z. Ren, Acta Materialia 2016, 102, 17.

[6] Z. Liu, Y. Wang, J. Mao, H. Geng, J. Shuai, Y. Wang, R. He, W. Cai, J. Sui, Z. Ren, Advanced Energy Materials 2016, 6, 1502269.

[7] J. P. Perdew, K. Burke, M. Ernzerhof, Phys. Rev. Lett 1996, 77, 3865.

[8] J. P. Perdew *et al.*, *J Phys Condens Matter* 2009, 21, 39.

[9] H. Akai, P. H. Dederichs, *Phys Rev B Condens Matter* 1983, 47, 8739-8747.

[10] H. Akai, Phy*s. Rev. Lett* 1988, 81, 3002.

[11] V. L. Moruzzi, J. F, Janak, and A. R. Williams, Calculated Electronic Properties of Metals (Pergamon, New York, 1978).

[12] S. Zhang, S.-H. Wei, A. Zunger, H. Katayama-Yoshida, Physical Review B 1998, 57, 9642.

[13] M. Lannoo, *Point defects in semiconductors I: theoretical aspects*, Vol. 22, Springer Science & Business Media, 2012.
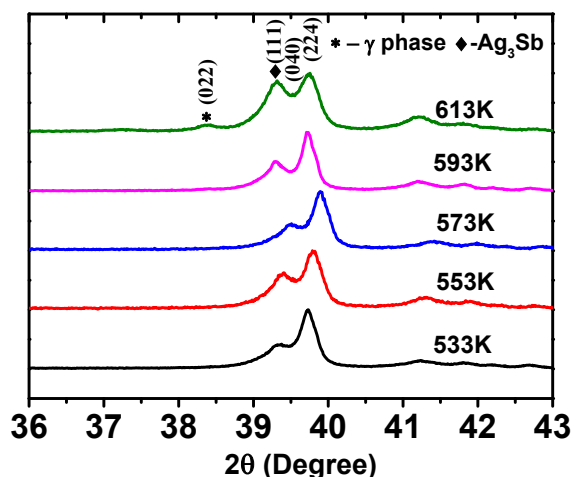
Figure S1. The enlarged XRD patterns of hot pressed $MgAg_{0.97}Sb_{0.99}$ samples at different temperatures (T = 533 K, 553 K, 573 K, 593 K, and 613 K).
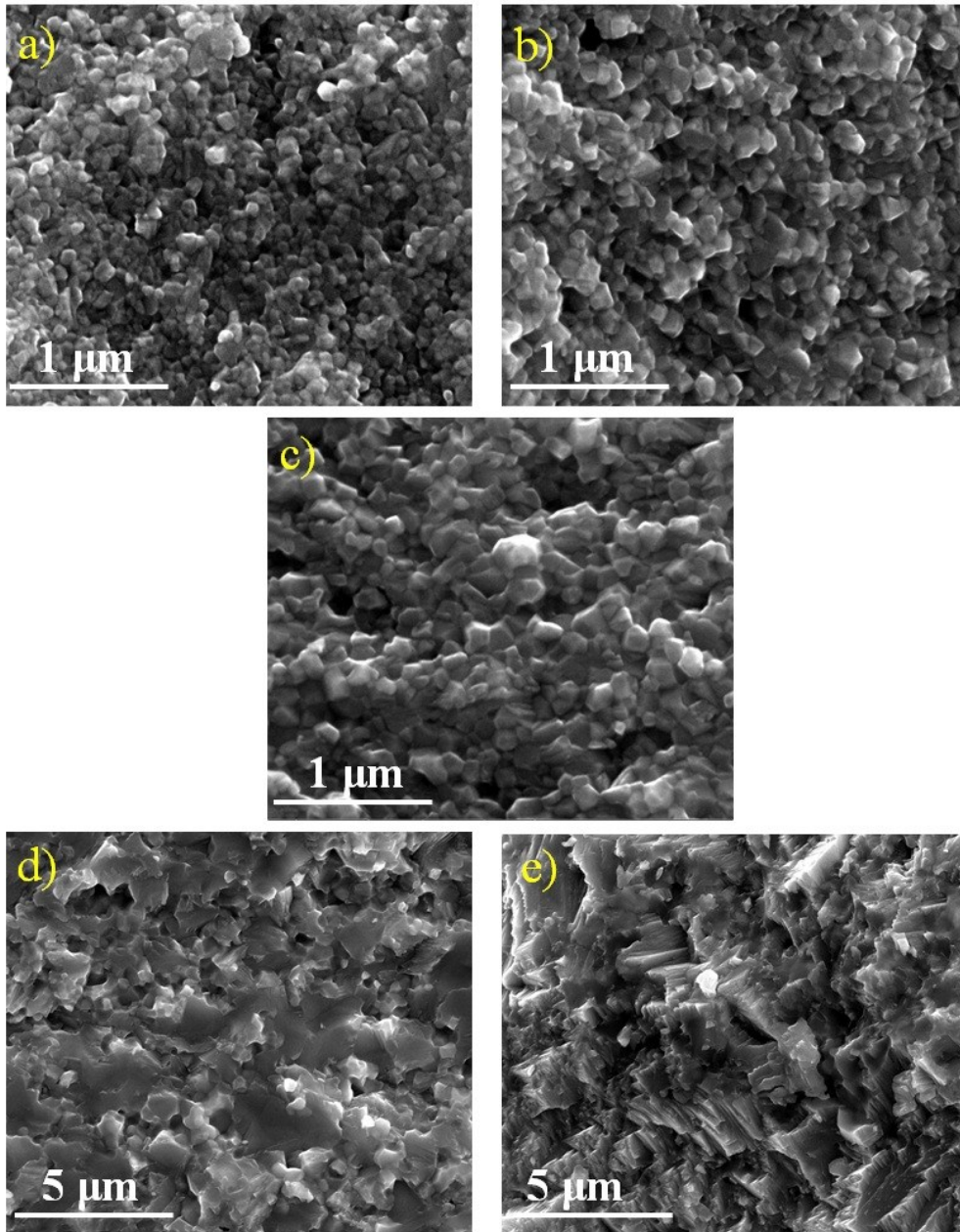
Figure S2. (a) - (e) Microstructure evolution of MgAg$_{0.97}$Sb$_{0.99}$ samples hot pressed at 533K, 553K, 573K, 593K and 613K, respectively.
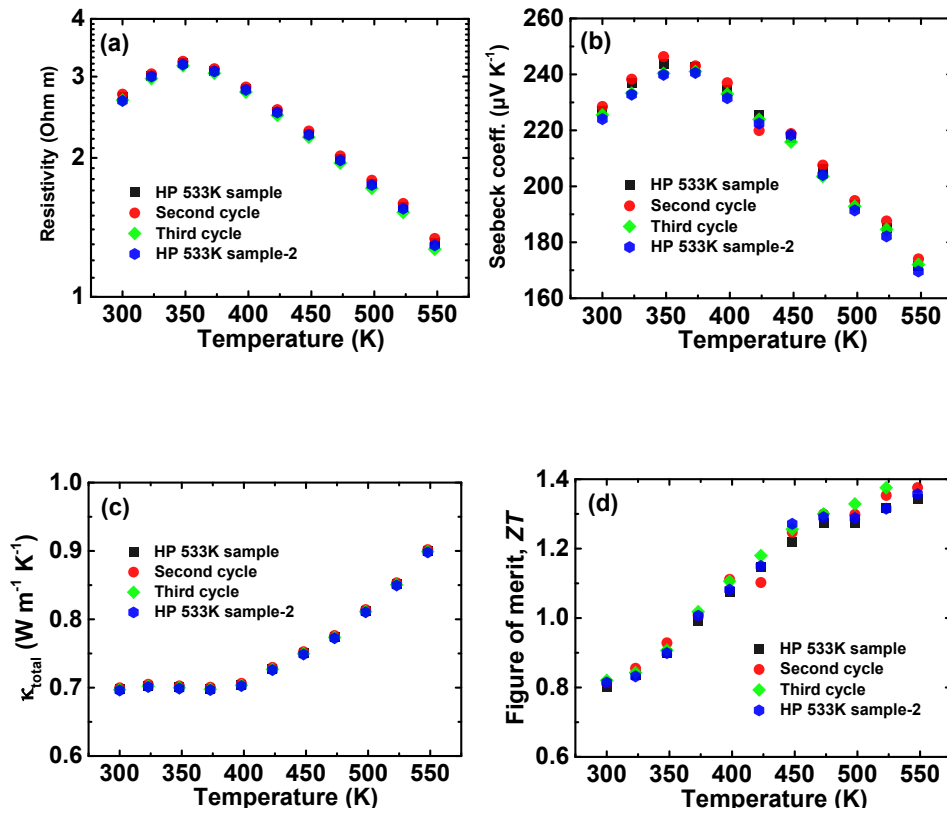
Figure S3. The thermal stability and repeatability of $MgAg_{0.97}Sb_{0.99}$ sample hot pressed at 533K. (a) Electrical resistivity, (b) Seebeck coefficient, (c) total thermal conductivity and (d) *ZT* values dependence of temperature.